Journal of the Nigerian Mathematical Society
Vol. 40, Issue 3, pp. 269-300, 2021

LOCAL NONSIMILARITY SOLUTION OF CASSON FLUID FLOW ALONG A STRETCHING SURFACE IN THE PRESENCE OF VISCOUS DISSIPATION, VARIABLE VISCOSITY AND THERMAL CONDUCTIVITY

M. O. LAWAL[1] AND S. O. AJADI

ABSTRACT.The study of heat and mass transfer of Casson fluid flow along a stretching sheet in the presence of viscous dissipation, variable viscosity and thermal conductivity is investigated. The governing partial differential equations are reduced to a system of coupled nonlinear quasi-ordinary differential equations through Sparrow-Quack-Boerner Local Nonsimilarity Method evaluated at a particular streamwise location by Midpoint method based on Richardson Extrapolation Enhancement scheme implemented on MAPLE 17 platform. The numerical results for velocity, temperature and concentration distributions as well as skin friction coefficient, Nusselt and Sherwood numbers were obtained. Parametric analysis of some embedded parameters such as Eckert number, Casson, thermal radiation and magnetic strength were carried out and these results have been displayed graphically. It is observed that the velocity, temperature and concentration profiles increase with increase in variable viscosity but the converse is true for the variable thermal conductivity.

Keywords and phrases: Casson fluid, local nonsimilarity, viscous dissipation, variable thermal conductivity, variable viscosity.
2010 Mathematical Subject Classification: 35G61, 76D05 76N10, 78M25, 76W05

1. INTRODUCTION

The study of non-Newtonian fluids characterized by nonlinear relationship between stress and rate of strain are well documented in the literature. Some examples of non-Newtonian fluids are Jeffery fluid [1] - [2], Maxwell fluid, Williamson fluid, Oldrody B fluid, Johnson-Segalman fluid, Viscoelastic fluid etc.

Received by the editors September 10, 2021; Revised: November 26, 2021; Accepted: December 03, 2021
www.nigerianmathematicalsociety.org; Journal available online at https://ojs.ictp.it/jnms/
[1]Corresponding author

There is another non-Newtonian fluid called Casson fluid, which became more popular in recent years in the study of non-Newtonian fluids due to its importance in many devices such as magnetohydrodynamic (MHD) power generators, MHD pumps, aerodynamics heating, polymer extrusion, petroleum industry, pharmaceutical process, purification of crude oil, fluid droplet sprays, metal forming, wire and glass fiber drawing and several others.

Casson [3] examined the validity of the Casson fluid model in his studies concerning the flow characteristics of blood. He reported that at low shear rates, the yield stress for blood is nonzero. Based on this concept, Mustafa [4] reported the unsteady boundary layer flow of Casson fluid on a moving surface to further explain the Casson fluid model. Dash *et al*. [5] defined Casson fluid as a shear thinning liquid which is assumed to have an infinite viscosity at zero rate of shear: a yield stress below which no flow occurs,and a zero viscosity at an infinite rate of shear. Models [1]-[2] have been proposed to clarify all the physical behaviors of Casson fluids. Some examples of Casson fluids include jelly, ketchup, custard, toothpaste, molten chocolate, yoghurt, maizena, paint, shampoo, tomato sauce, honey, soup, suspension or solution of clay, starch or graphite and human blood.

A boundary layer analysis was presented by Mukhopadhyay *et al*. [6] for non-Newtonian fluid flow and heat transfer over a nonlinearly stretching surface where it is noted that the Casson fluid model is used to characterize the non-Newtonian fluid behaviour. The process of suction or blowing has also its importance in many engineering activities for example, in the design of thrust bearing and radial diffusers, and thermal oil recovery. Suction or injection (blowing) of a fluid through the bounding surface can significantly change the flow field. Suction is applied to chemical processes to remove reactants whereas blowing is used to add reactant, cool the surface, prevent corrosion or scaling and reduce the drag.

In the same vein, Mukhopadhyay [7] numerically examined the boundary layer flow due to an exponentially stretching surface in the presence of an applied magnetic field. It was found that the effect of increasing values of the Casson parameter is to suppress the velocity field. However the temperature is enhanced when Casson parameter increases. Shateyi *et al*. [8] investigated Casson fluid flow in the presence of free convection of combined heat and mass transfer toward an unsteady permeable stretching sheet with thermal radiation, viscous dissipation and chemical reaction. The equations were solved numerically using Runge-Kutta-Fehlberg method for different values of parameters such as magnetic parameter, radiation parameter, chemical reaction parameter, suction/injection parameter and Eckert number.

Nadeem *et al.* [9] investigated MHD three-dimensional Casson fluid flow past a porous linearly stretching sheet for momentum equation adopting fourth-order Runge-Kutta-Fehlberg method with a shooting technique. Pramanik [10] studied Casson fluid flow and heat transfer past an exponentially porous stretching surface in presence of thermal radiation applying the fourth order classical Runge-Kutta method. Ramesh and Devakar [11] presented some analytical solutions for flows of Casson fluid with slip boundary conditions where they studied three fundamental flows namely Couette, Poiseuille and generalized Couette flows of an incompressible Casson fluid between parallel plates using slip boundary conditions.

Afikuzzaman [12] presented MHD Casson fluid flow through a parallel plate under the action of mass transfer by using implicit finite difference method has been taken into consideration. The physical properties are graphically discussed for different values of corresponding parameters. Arthur *et al.* [13] analyzed Casson fluid flow over a vertical porous surface with chemical reaction in the presence of magnetic field. A similarity analysis was used to transform the system of partial differential equations describing the problem into ordinary differential equations. The reduced system was solved using the Newton-Raphson shooting method alongside the forth-order Runge-Kutta algorithm.

Many boundary layer flow and contemporary heat transfer problem of interest are not admissible to similarity solutions. According to White [14], the coordinates x, y must disappear through suitable transformation in the transformed equations of a similar problem otherwise, the problem is not self similar or locally similar. However, Sparrow *et al.* [15] stated that nonsimilarity boundary layer may stem from a variety of causes such as variation in the wall temperature, variation in free-stream velocity, surface mass transfer, effect of suction or injection of fluid at the wall, buoyancy force effect, inclination angle effect etc. Mohamad *et al.* [16] observed that the nonsimilarity of boundary layer can also arise from more than one factor while investigating the combined heat and mass transfer on mixed convection non-similar flow of electrically conducting nanofluid along a permeable vertical plate in the presence of thermal radiation.

There are various numerical methods proposed to deal with such nonsimilar boundary layer problems, the most popular among them is the local nonsimilarity method initiated by Sparrow *et al.* [15]. This is described and applied for treating nonsimilar boundary layer problems in which all terms appearing in the conservation equations are retained without approximation but are selectively neglected in the derived subsidiary equations. This present research considered some thermo-physical parameters in which buoyancy effect, surface mass transfer and pressure gradient are included therefore making the problem not admissible to local similarity solution approach or that any solution obtained will be of uncertain accuracy. Hence, the adoption of the local nonsimilarity approach.

Ibrahim and Hassanien [17] carried out analysis to study the heat transfer characteristics of laminar mixed convection boundary layer flow of a micropolar fluid over a semi-infinite horizontal flat plate with nonuniform surface temperature. The effect of material parameter, the exponent for the power-law variation in wall temperature and the nonsimilar mixed convection parameter are considered. The boundary layer equations were solved numerically by means of finite difference method with different correction. Patil *et al*. [18] obtained non-similar solutions for steady two dimensional double diffusive mixed convection boundary layer flows over an impermeable exponentially stretching sheet in an exponentially moving free stream under the influence of chemically reactive species using an implicit finite difference scheme in combination with the Newtons linearization technique.

Animasahun *et al*. [19] investigated the behaviour of Casson fluid flow with variable thermo-physical property along exponentially stretching sheet with suction and exponentially decaying internal heat generation using the homotopy analysis method.

The objective of the present study is to obtain Local Nonsimilarity Solution of MHD Mixed Convective Casson Fluid Flow along a Stretching Sheet in the Presence of Viscous Dissipation, Variable Viscosity and Thermal Conductivity. To the best of the authors' knowledge, the investigation on Casson Fluid along a Stretching Surface in the Presence of Variable Viscosity and Thermal Conductivity using Local Nonsimilarity approach have not been carried out.

The governing equations modelling MHD flow, heat and mass transfer over stretching surfaces are highly nonlinear therefore making exact solutions impossible to obtain. Therefore, numerical solutions have always been developed and modified with the aim of getting more accurate and stable solutions. This present work seeks to obtain Local Nonsimilarity Solution(LNS) of MHD mixed convective Casson fluid flow along a stretching sheet in the presence of viscous dissipation, variable viscosity and thermal conductivity employing Midpoint

Method based on Richardson Extrapolation Enhancement scheme implemented on the MAPLE 17 platform.

1.2 Research Questions

Based on the aforementioned, the following research questions are appropriate:

(i) Does the viscous dissipation have effect on Casson fluid stretching surface?
(ii) What are the contributions of variable viscosity and thermal conductivity?
(iii) What is the influence of nonlinear stretching velocity? and
(iv) Why the need for Local Nonsimilarity Solution Approach?

2. FORMULATION OF THE PROBLEM

Consider heat and mass transfer of an incompressible two-dimensional unsteady laminar boundary layer flow of Casson fluid over a stretching sheet with viscous dissipation, thermal radiation, variable viscosity and thermal conductivity. The rheological equation of an isotropic and incompressible flow of a Casson fluid (Mustafa *et al*. [4]) is given by:

$$\tau^{1/n} = \tau_0^{1/n} + \mu\dot{\gamma}^{1/n}. \tag{1}$$

It can also take the form (Nakamura and Sawada [2])

$$\tau_{ij} = \left[\mu_B + \left(\frac{P_y}{\sqrt{2\pi}}\right)^{1/n}\right]^n 2e_{ij}. \tag{2}$$

Different values of the flow index n are used in rheological application. For example, chocolate and blood flow system, $n = 2$. However, in this paper, and for obvious reason, we take $n = 1$. Therefore,

$$\begin{aligned} \tau_{ij} &= 2e_{ij}\left(\mu_B + \frac{P_y}{\sqrt{2\pi}}\right) \text{ when } \pi > \pi_c, \\ \tau_{ij} &= 2e_{ij}\left(\mu_B + \frac{P_y}{\sqrt{2\pi_c}}\right) \text{ when } \pi < \pi_c, \end{aligned} \tag{3}$$

where P_y is known as yield stress of the fluid, mathematically expressed as $P_y = \frac{\mu_B\sqrt{2\pi}}{\beta}$ then, e_{ij} is the (i, j)th component of the deformation rate, μ_B is known as plastic dynamic viscosity of the non-Newtonian fluid, $\pi = e_{ij}e_{ij}$ is the product of the component of deformation rate with itself and π_c is the critical value based on the non-Newtonian model. For Casson fluid (Non Newtonian) flow, where $\pi > \pi_c$, it is possible to say that

$$\mu = \mu_B + \frac{P_y}{\sqrt{2\pi}}. \tag{4}$$

Substituting P_y into (4), the kinematics viscosity of Casson fluid is now depending on plastic dynamic viscosity μ_B, density ρ and Casson parameter β,

$$\nu = \frac{\mu_B}{\rho}\left(1 + \frac{1}{\beta}\right). \tag{5}$$

Furthermore, the temperature dependent viscosity and thermal conductivity are respectively given as (Mukhopadhyay *et al*. [6]; Animasahun *et al*. [19]; Bhattacharyya *et al*. [20]; Prasad *et al*. [21])

$$\mu(T) = \mu^*[b + r(T_w - T)] \quad \text{and} \quad \kappa(T) = \kappa^*[d + \epsilon(T_w - T)], \tag{6}$$

where μ^* and κ^* are the coefficients of viscosity and thermal conductivity respectively in the free stream $r = r^*(T_w - T_\infty)$ and $\epsilon = \epsilon^*(T_w - T_\infty)$. Also b, d, r and ϵ are constant. We consider the case when $b = d = 1$ and $r, \epsilon^* > 0$.

Extending Shateyi [8] and Mukhopadhyay [7] among others, introducing the boundary layer approximations, the MHD heat and mass transfer fluid flows are governed by the following conservative equations written as:

$$\frac{\partial u}{\partial x} + \frac{\partial v}{\partial y} = 0, \tag{7}$$

$$\begin{aligned}\frac{\partial u}{\partial t} + u\frac{\partial u}{\partial x} + v\frac{\partial u}{\partial y} =& \frac{1}{\rho}\left(1 + \frac{1}{\beta}\right)\frac{\partial}{\partial y}\left(\mu(T)\frac{\partial u}{\partial y}\right) - \frac{1}{\rho}\frac{\partial P}{\partial x}\\ &+ g\beta_T(T - T_\infty) + g\beta_c(C - C_\infty) - \frac{\sigma B^2}{\rho}u,\end{aligned} \tag{8}$$

$$\begin{aligned}\frac{\partial T}{\partial t} + u\frac{\partial T}{\partial x} + v\frac{\partial T}{\partial y} =& \frac{1}{\rho C_p}\left(1 + \frac{1}{\beta}\right)\frac{\partial}{\partial y}\left(\kappa(T)\frac{\partial u}{\partial y}\right)\\ &+ \frac{\mu(T)}{\rho}\left(1 + \frac{1}{\beta}\right)\left(\frac{\partial u}{\partial y}\right)^2 - \frac{1}{\rho C_p}\frac{\partial q_r}{\partial y} + \frac{\sigma B^2}{\rho}u^2,\end{aligned} \tag{9}$$

$$\frac{\partial C}{\partial t} + u\frac{\partial C}{\partial x} + v\frac{\partial C}{\partial y} = \frac{D_m}{\rho C_p}\frac{\partial^2 C}{\partial y^2} - K_r(C - C_\infty). \tag{10}$$

The associated initial and boundary conditions for the present problem are

$$t = 0: \;\; u = 0, \;\; v = 0, T = T_w, \;\; C = C_w \text{ at } y \geq 0, \tag{11}$$

$$t > 0: \;\; u = U_w(x,t), \;\; v = V_w, T = T_w, \;\; C = C_w \text{ at } y = 0, \tag{12}$$

$$t > 0: \ u = U_e(x,t), \ w \to 0, \ T \to T_\infty, \ C \to C_\infty \text{ as } y \to \infty. \quad (13)$$

Local Nonsimilarity Method

Problems involving mixed convection in boundary layers analysis are usually not self similar or locally similar because the embedded parameters are not independent of the original variables. The implementation of local nonsimilarity method as detailed in Minkowycz and Sparrow [22] involves the execution of a definite succession of steps which starts with the transformation of coordinates. The first step in the development of the solution method is to transform the problem from the x, y coordinate system to the ξ, η system. The coordinate η, which involves both x and y, with x denoting the streamwise coordinate and y the transverse coordinate, may be termed a pseudo-similarity variable; it is chosen to reduce to a true similarity variable for boundary layers which are similar. In the same vein, ξ is related to x alone and is so chosen that x does not appear explicitly in the transformed conservation equations or the boundary conditions. Following Sparrow and Yu [23], Ishak *et al*. [24] and Khan *et al*. [25], we devise the following dimensionless velocity quantities and parameters as functions of f, θ and ϕ and in accordance with the foregoing, η and ξ for the problem of uniform-surface mass transfer:

$$\begin{aligned}
&\psi = \sqrt{\frac{\lambda \nu b}{1-ct}} x^{\frac{j+1}{2}} f(\xi,\eta), \ \eta = \sqrt{\frac{\lambda b}{\nu(1-ct)}} y x^{\frac{j-1}{2}}, \ \xi = x, \\
&U_e = \frac{\lambda a x^j}{1-ct}, \theta = \theta(\xi,\eta) = \frac{T - T_\infty}{T_w - T_\infty}, \ \phi = \phi(\xi,\eta) = \frac{C - C_\infty}{C_w - C_\infty}, \\
&U_w = \frac{\lambda b x^j}{1-ct}, B^2 = \frac{B_0^2}{1-ct}.
\end{aligned} \quad (14)$$

The introduction of the power of x follows from Kundu [26]. If $j = 1 = \lambda$, (14) reduces to Shateyi *et al*. [8] among others in the literature, where b is stretching rate, t is the time and j is a numerical exponent associated with pressure gradient parameter. λ is a scaling parameter of the dimension L^{1-j} and $L \neq 0$.

Due to the adopted nonlinear unsteady stretching sheet velocity from Kundu [26], Lawal and Ajadi [27], Shateyi *et al*. [8] and Thumma *et al*. [28], the dimensionally balanced and homogeneous surface temperature and concentration of the sheet which varies with the distance x, y and time t take the form:

$$T_w = T_\infty + T_0 \frac{\lambda^2 b x^{2j}}{2\nu(1-ct)^{3/2}}, \ C_w = C_\infty + C_0 \frac{\lambda^2 b x^{2j}}{2\nu(1-ct)^{3/2}}. \quad (15)$$

The expressions $U_w(x,t)$, $U_e(x,t)$, $T_w(x,t)$, $C_w(x,t)$ are valid only for the time $t < \frac{1}{c}$ (i.e. $ct < 1$) and $c > 0$ (positive constant). T_0 is the reference temperature such that $0 \leq T_0 \leq T_w$.

By using the Rosseland approximation [29, 30], the radiative heat flux is given by

$$q_r = -\frac{4\sigma^*}{3K^*}\frac{\partial T^4}{\partial y}, \tag{16}$$

where σ^* and K^* are the Stefan-Boltzman constant and the Rosseland mean absorption coefficient respectively. We assume that the temperature differences within the flow are sufficiently small such that T^4 may by expressed as a linear function of temperature. Expanding T^4 in a Taylor series about T_∞ and neglecting higher order terms we obtain

$$T^4 \approx 4T_\infty^3 T - 3T_\infty^4. \tag{17}$$

Using (16) and (17) in the third term on the right hand side of equation (9) we obtain

$$\frac{\partial q_r}{\partial y} = -\frac{16\sigma^*}{3K^*}\frac{\partial^2 T}{\partial y^2}. \tag{18}$$

Introducing the stream function ψ, the velocity components u and v can be written as

$$u = \frac{\partial \psi}{\partial y} \text{ and } v = -\frac{\partial \psi}{\partial x}, \tag{19}$$

and thus the continuity equation (7) is automatically satisfied.
By applying these similarity variables and quantities above in (14) and (15), the governing partial differential equations are transformed into a system of coupled non-linear ordinary differential equations as:

$$\begin{aligned} &[1+\epsilon-\theta\epsilon]\left(1+\frac{1}{\beta}\right)f''' - \epsilon\left(1+\frac{1}{\beta}\right)\theta' f'' + \frac{j+1}{2}ff'' \\ &+ j\left(\omega - (f')^2\right) - A\left(f' + \frac{1}{2}\eta f''\right) + Gr_\xi\theta + Gc_\xi\phi - Mf' \\ &= \xi\left[f'\frac{\partial f'}{\partial \xi} - f''\frac{\partial f}{\partial \xi}\right], \end{aligned} \tag{20}$$

$$\begin{aligned} &\frac{1}{Pr}(1+r\theta+\frac{4}{3}R)\theta'' + \frac{r}{Pr}\theta'^2 + \left(\frac{j+1}{2}f - \frac{A}{2}\eta\right)\theta' \\ &- \left(2jf' + \frac{3A}{2}\right)\theta + Ec\left[(1+\epsilon-\theta\epsilon)\left(1+\frac{1}{\beta}\right)f''^2 + Mf'^2\right] \\ &= \xi\left[f'\frac{\partial \theta}{\partial \xi} - \theta'\frac{\partial f}{\partial \xi}\right], \end{aligned} \tag{21}$$

$$\frac{1}{Sc}\phi'' + \left(\frac{j+1}{2}f - \frac{A}{2}\eta\right)\phi' - \left(2jf' + \frac{3A}{2} + LrRe_x\right)\phi = \xi\left[f'\frac{\partial\phi}{\partial\xi} - \phi'\frac{\partial f}{\partial\xi}\right]. \tag{22}$$

The corresponding dimensionless initial and boundary conditions are

$$f(\xi,0) = f_w, f'(\xi,0) = 1,\ \theta(\xi,0) = 1,\ \phi(\xi,0) = 1, \tag{23}$$

$$f'(\xi,\infty) = \omega,\ \theta(\xi,\infty) = 0,\ \phi(\xi,\infty) = 0, \tag{24}$$

where primes denote the differentiation with respect to η, θ is the dimensionless temperature, ϕ is the dimensionless concentration, $Pr = \frac{\mu C_p}{\kappa}$, $Sc = \frac{\nu}{D}$, $A_\xi = \frac{c}{\lambda b\xi^{j-1}}$, $M = \frac{\sigma B_0^2}{\rho b}$, $R = \frac{4\sigma^* T_\infty^3}{K_s K}$, $Gr_\xi = \frac{g\beta_T(T_w - T_\infty)\xi}{U_w^2}$, $Gc_\xi = \frac{g\beta_c(C_w - C_\infty)\xi}{U_w^2}$, $Lr = \frac{Kr(1-ct)}{b\xi^{j-1}}$, $\omega = \frac{a}{b}$, $Ec = \frac{U_e^2}{C_p(T_w - T_\infty)}$. If $f(0) = f_w$ then $V_w = -(\frac{\nu U_w}{\xi})^{\frac{1}{2}}f(0)$ represents the mass transfer at the surface where $f_w < 0$ for injection and $f_w > 0$ for suction.

In obtaining the local nonsimilarity solutions of equations (20) - (22), the appearance of the terms $\partial/\partial\xi$ may be changed for the next level of truncation by defining the new dependent variables as $\frac{\partial f}{\partial\xi} = F$, $\frac{\partial\theta}{\partial\xi} = X$ and $\frac{\partial\phi}{\partial\xi} = Y$.

First Level of Truncation (Local Similarity)

The respective right hand side (RHS) terms of equations (20) - (22) $\xi\left[f'F' - Ff''\right]$, $\xi\left[f'X - F\theta'\right]$ and $\xi\left[f'Y - F\phi'\right]$ are deleted which coincides with equations for local similarity approach.

$$[1+\epsilon-\theta\epsilon]\left(1+\frac{1}{\beta}\right)f''' - \epsilon\left(1+\frac{1}{\beta}\right)\theta' f'' + \frac{j+1}{2}ff'' + j\left(\omega - (f')^2\right) - A\left(f' + \frac{1}{2}\eta f''\right) + Gr_\xi\theta + Gc_\xi\phi - Mf' = 0, \tag{25}$$

$$\frac{1}{Pr}\left(1 + r\theta + \frac{4}{3}R\right)\theta'' + \frac{r}{Pr}\theta'^2 + \left(\frac{j+1}{2}f - \frac{A}{2}\eta\right)\theta' - \left(2jf' + \frac{3A}{2}\right)\theta + Ec\left[(1+\epsilon-\theta\epsilon)\left(1+\frac{1}{\beta}\right)f''^2 + Mf'^2\right] = 0, \tag{26}$$

$$\frac{1}{Sc}\phi'' + \left(\frac{j+1}{2}f - \frac{A}{2}\eta\right)\phi' - \left(2jf' + \frac{3A}{2} + LrRe_x\right)\phi = 0. \qquad (27)$$

Second Level of Truncation

The governing equations for f, θ and ϕ at this level of truncation in equations (20) - (22) are retained without approximation. The auxiliary equations for F, X and Y are derived by taking $\frac{\partial}{\partial \xi}$ of (20) - (22),

$$\begin{aligned}
&[1+\epsilon-\theta\epsilon]\left(1+\frac{1}{\beta}\right)F''' - \epsilon\left(1+\frac{1}{\beta}\right)X'f'' - \epsilon\left(1+\frac{1}{\beta}\right)\theta'F'' \\
&+ \frac{j+1}{2}\left[fF'' + Ff''\right] - 2jF'f' - A\left(F' + \frac{1}{2}\eta F''\right) + Gr_\xi X \\
&+ Gc_\xi Y - MF' = f'F' - Ff'' + \xi\left[\frac{\partial}{\partial \xi}\left(f'F' - Ff''\right)\right],
\end{aligned} \qquad (28)$$

$$\begin{aligned}
&\frac{1}{Pr}\left(1 + r\theta + \frac{4}{3}R\right)X'' + \frac{r}{Pr}2X'\theta'^2 + \left(\frac{j+1}{2}f - \frac{A}{2}\eta\right)X \\
&+ \frac{j+1}{2}F\theta' - \left(2jf' + \frac{3A}{2}\right)X - (2jF')\theta \\
&+ Ec\left[(1+\epsilon-\theta\epsilon)\left(1+\frac{1}{\beta}\right)(2f''F'') + 2Mf'F'\right] \\
&= f'X - F\theta' + \xi\left[\frac{\partial}{\partial \xi}\left(f'X - F\theta'\right)\right],
\end{aligned} \qquad (29)$$

$$\begin{aligned}
&\frac{1}{Sc}Y'' + \left(\frac{j+1}{2}f - \frac{A}{2}\eta\right)Y' - \left(\frac{3A}{2} + 2jf' + LrRe_x\right)Y \\
&+ \frac{j+1}{2}F\phi' - 2jF'\phi = f'Y - F\phi' + \xi\left[\frac{\partial}{\partial \xi}(f'Y - F\phi')\right].
\end{aligned} \qquad (30)$$

Third Level of Truncation

The governing equations for F, X and Y at this level of truncation in equations (28) - (30) are retained without approximation. The auxiliary equations for G, H and S are derived by taking $\frac{\partial}{\partial \xi}$ of (28) - (30), introducing $\frac{\partial F}{\partial \xi} = G$, $\frac{\partial X}{\partial \xi} = H$ and $\frac{\partial Y}{\partial \xi} = S$ and then respectively deleting the terms $\frac{\partial^2}{\partial \xi^2}\left(f'F' - f''F\right)$, $\frac{\partial^2}{\partial \xi^2}\left(f'X - \theta'F\right)$ and

$\dfrac{\partial^2}{\partial \xi^2}(f'Y-\phi' F)$. According to this concept as reported by Sparrow *et al*. [15] and Mohamad *et al*. [16], the RHS of the equations are assumed to be sufficiently small so that it may be approximated by zero. Boundary conditions for F, X and Y are also obtained by differentiating (28) and (30) with respect to ξ and deleting $\dfrac{\partial G}{\partial \xi}$, $\dfrac{\partial H}{\partial \xi}$ and $\dfrac{\partial S}{\partial \xi}$.

$$\begin{aligned}
&[1+\epsilon-\theta\epsilon]\left(1+\frac{1}{\beta}\right)G'''-\epsilon\left(1+\frac{1}{\beta}\right)(X'F''+H'f'')\\
&-\epsilon\left(1+\frac{1}{\beta}\right)(\theta' G''+X'F'')-\epsilon\left(1+\frac{1}{\beta}\right)\theta' F''\\
&+\frac{j+1}{2}[fG''+Ff''+f''G+F'F]-2j(F'F'+G'f')\\
&-A\left(G'+\frac{1}{2}\eta G''\right)+Gr_\xi H+Gc_\xi S-MG'-f'G'+(F')^2\\
&+(f''G-F''F)=\xi\left[\frac{\partial^2}{\partial\xi^2}(f'F'-Ff'')\right],
\end{aligned}\tag{31}$$

$$\begin{aligned}
&\frac{1}{Pr}(1+r\theta+\frac{4}{3}R)H''+\frac{2r}{Pr}\left(X'^2+\theta' H'\right)+\left(\frac{j+1}{2}f-\frac{A}{2}\eta\right)H'\\
&+\frac{j+1}{2}(FX'+G\theta')-\left(2jf'+\frac{3A}{2}\right)H-2j(X'^2+H\theta)\\
&-2jF'X+Ec\left[(1+\epsilon-\theta\epsilon)\left(1+\frac{1}{\beta}\right)2(F''F''+f''G'')\right]\\
&+2MEc\left(f'G'+F'^2\right)=f'H+F'X-(\theta' G+X'F)\\
&+\xi\left[\frac{\partial^2}{\partial\xi^2}(f'X-F\theta')\right],
\end{aligned}\tag{32}$$

$$\begin{aligned}
&\frac{1}{Sc}S''+\left(\frac{j+1}{2}f-\frac{A}{2}\eta\right)S'-\left(\frac{3A}{2}+2jf'+LrRe_x\right)S\\
&+\frac{j+1}{2}FY'+\frac{j+1}{2}(FY'+G\phi')-2jF'Y-2j(F'Y+G'\phi)\\
&-(f'S-F'Y)+(FY'-G\phi')=\xi\left[\frac{\partial^2}{\partial\xi^2}(f'Y-F\phi')\right].
\end{aligned}\tag{33}$$

The governing equations and its auxiliary equation are therefore brought together as

$$\begin{aligned}
&[1+\epsilon-\theta\epsilon]\left(1+\frac{1}{\beta}\right)f'''-\epsilon\left(1+\frac{1}{\beta}\right)\theta' f''+\frac{j+1}{2}ff'' \\
&+j\left(\omega-(f')^2\right)-A\left(f'+\frac{1}{2}\eta f''\right)+Gr_\xi\theta+Gc_\xi\phi-Mf' \\
&=\xi\left[f'F'-Ff''\right],
\end{aligned} \tag{34}$$

$$\begin{aligned}
&\frac{1}{Pr}\left(1+r\theta+\frac{4}{3}R\right)\theta''+\frac{r}{Pr}\theta'^2+\left(\frac{j+1}{2}f-\frac{A}{2}\eta\right)\theta' \\
&-\left(2jf'+\frac{3A}{2}\right)\theta+Ec\left[(1+\epsilon-\theta\epsilon)\left(1+\frac{1}{\beta}\right)f''^2+Mf'^2\right] \\
&=\xi\left[f'X-F\theta'\right],
\end{aligned} \tag{35}$$

$$\begin{aligned}
&\frac{1}{Sc}\phi''+\left(\frac{j+1}{2}f-\frac{A}{2}\eta\right)\phi'-\left(2jf'+\frac{3A}{2}+LrRe_x\right)\phi \\
&=\xi\left[f'Y-F\phi'\right].
\end{aligned} \tag{36}$$

$$\begin{aligned}
&[1+\epsilon-\theta\epsilon]\left(1+\frac{1}{\beta}\right)F'''-\epsilon X\left(1+\frac{1}{\beta}\right)f'''+\epsilon\left(1+\frac{1}{\beta}\right)X'f'' \\
&-\epsilon\left(1+\frac{1}{\beta}\right)\theta' F''+\frac{j+1}{2}\left[fF''+Ff''\right]-j\left(2F'f'\right) \\
&-A\left(F'+\frac{1}{2}\eta F''\right)+Gr_\xi X+Gc_\xi Y-MF'=f'F'-Ff'' \\
&+\xi\left[f'G'+(F')^2-(f''G+F''F)\right],
\end{aligned} \tag{37}$$

$$\begin{aligned}
&\frac{1}{Pr}(1+r\theta+\frac{4}{3}R)X''+\frac{rX}{Pr}\theta''+\frac{r}{Pr}2X'\theta'^2 \\
&+\left(\frac{j+1}{2}f-\frac{A}{2}\eta\right)X'+\frac{j+1}{2}F\theta'-\left(2jf'+\frac{3A}{2}\right)X \\
&-(2jF')\theta+Ec\left[(1+\epsilon-\theta\epsilon)\left(1+\frac{1}{\beta}\right)(2f''F'')+2Mf'F'\right] \\
&=f'X-F\theta'+\xi\left[f'H+F'X-(\theta'G+X'F)\right],
\end{aligned} \tag{38}$$

$$\begin{aligned}
&\frac{1}{Sc}Y''+\left(\frac{j+1}{2}f-\frac{A}{2}\eta\right)Y'-\left(\frac{3A}{2}+2jf'+LrRe_x\right)Y+\frac{j+1}{2}F\phi' \\
&-2jF'\phi=f'Y-F\phi'+\xi\left[f'S+F'Y-(FY'+G\phi')\right].
\end{aligned} \tag{39}$$

$$
\begin{aligned}
&[1+\epsilon-\theta\epsilon]\left(1+\frac{1}{\beta}\right)G''' - \epsilon\left(1+\frac{1}{\beta}\right)(XF''' + Hf''') \\
&- \epsilon\left(1+\frac{1}{\beta}\right)(X'F'' + H'f'') - \epsilon\left(1+\frac{1}{\beta}\right)(\theta'G'' + X'F'') \\
&- \epsilon\left(1+\frac{1}{\beta}\right)\theta'F'' + \frac{j+1}{2}[fG'' + Ff'' + f''G + F'F] \\
&- 2j(F'F' + G'f') - A\left(G' + \frac{1}{2}\eta G''\right) + Gr_{\xi}H + Gc_{\xi}S - MG' \\
&- f'G' + (F')^2 + (f''G - F''F) = 0,
\end{aligned} \tag{40}
$$

$$
\begin{aligned}
&\frac{1}{Pr}\left(1+r\theta+\frac{4}{3}R\right)H'' + \frac{r}{Pr}(XX'' + H\theta'') + \frac{2r}{Pr}\left(X'^2 + \theta'H'\right) \\
&+ \left(\frac{j+1}{2}f - \frac{A}{2}\eta\right)H' + \frac{j+1}{2}(FX' + G\theta') - \left(2jf' + \frac{3A}{2}\right)H \\
&- 2jF'X - 2j(X'^2 + H\theta) + 2MEc\left(f'G' + F'^2\right) - f'H - F'X \\
&+ Ec\left[(1+\epsilon-\theta\epsilon)\left(1+\frac{1}{\beta}\right)2(F''F'' + f''G'')\right] + (\theta'G + X'F) = 0,
\end{aligned} \tag{41}
$$

$$
\begin{aligned}
&\frac{1}{Sc}S'' + \left(\frac{j+1}{2}f - \frac{A}{2}\eta\right)S' - \left(\frac{3A}{2} + 2jf' + LrRe_x\right)S \\
&+ \frac{j+1}{2}FY' + \frac{j+1}{2}(FY' + G\phi') - 2jF'Y - 2j(F'Y + G'\phi) \\
&- (f'S - F'Y) + (FY' - G\phi') = 0.
\end{aligned} \tag{42}
$$

The corresponding dimensionless initial and boundary conditions are

$$
\begin{aligned}
&f(\xi,0) = f_w, f'(\xi,0) = 1, f'(\xi,\infty) = \omega, \\
&\theta(\xi,0) = 1, \theta(\xi,\infty) = 0, \phi(\xi,0) = 1, \phi(\xi,\infty) = 0,
\end{aligned} \tag{43}
$$

$$
\begin{aligned}
&F(\xi,0) = 0, F'(\xi,0) = 0, F'(\xi,\infty) = 0, \\
&X(\xi,0) = 0, X(\xi,\infty) = 0, Y(\xi,0) = 0, Y(\xi,\infty) = 0,
\end{aligned} \tag{44}
$$

$$
\begin{aligned}
&G(\xi,0) = 0, G'(\xi,0) = 0, G'(\xi,\infty) = 0, \\
&H(\xi,0) = 0, H(\xi,\infty) = 0, S(\xi,0) = 0, S(\xi,\infty) = 0.
\end{aligned} \tag{45}
$$

The physical quantities of engineering interest in this problem are the local Skin-friction coefficients (Cf_x), the local Nusselt number (Nu_x) and the local Sherwood number (Sh_x). Given the velocity field, the local Skin-friction coefficients on the sheet wall can be obtained in non-dimensional form as:

$$\begin{aligned} Cf_x &= -\frac{2\mu\left(\frac{\partial u}{\partial y}\right)_{y=0}}{\rho U_w^2} \quad \text{from which we obtain} \\ \frac{1}{2}\sqrt{Re_x}C_f &= -\left(1+\frac{1}{\beta}\right)f''(\xi,0). \end{aligned} \tag{46}$$

Given the temperature field, the rate of heat transfer coefficient can be obtained in the form

$$\begin{aligned} Nu_x &= \frac{xq_w}{\kappa(T_w - T_\infty)} \quad \text{from which we obtain} \\ \frac{1}{\sqrt{Re_x}}Nu_x &= -\left(1+\frac{4}{3}R\right)\theta'(\xi,0), \end{aligned} \tag{47}$$

where $q_w = \kappa\left(\frac{\partial T}{\partial y}\right)_{y=0} + (q_r)_w$ is the wall heat flux while $q_r = -\frac{16\sigma^*}{3K^*}T_\infty^3\frac{\partial T}{\partial y}$ (See Akinbobola and Okoya [31], Bataller [32] and Fatunmbi *et al*. [33] and Khan *et al*. [34]).

Also, given the concentration field, the rate of mass transfer coefficient can be obtained in non-dimensional form. The Sherwood number is thus given by

$$Sh_x = \frac{xq_w}{D(C_w - C_\infty)} \quad \text{from which we obtain } \frac{1}{\sqrt{Re_x}}Sh_x = -\phi'(\xi,0). \tag{48}$$

3. MATHEMATICAL SOLUTION

The governing equations reduced to non-linear coupled differential equations (34)-(45) with the boundary conditions (34)-(45) are not amenable to exact (analytical) solutions thus we resolve to numerical solution by employing Midpoint Method based on Richardson Extrapolation (MMRE) Enhancement scheme implemented on MAPLE 17 platform. The asymptotic boundary conditions (24) for η_{max} as follow:

$$\eta_{max} = 14, f'(14) = \theta(14) = \phi(14) = 0. \tag{49}$$

From this process of numerical computation, the skin-friction coefficient, the Nusselt number and Sherwoood number which correspond to $f''(0)$, $\theta'(0)$ and $\phi'(0)$ respectively are also obtained and their numerical values are presented in a tabular form.

4. RESULTS AND DISCUSSION

The basic target of this section is to examine the influences of physical parameters on the dimensionless axial and transverse velocities, the temperature and Casson fluid concentration. The computations have been carried out by assuming various values of the parameters involved in the problem and the results are illustrated through graphs. However, In a bid to validate the present solution, comparisons have been made with previously published data from the literature for the modified skin friction coefficient in Table 1 and excellent agreement is found.

From Table 1, we discovered that the modified skin friction coefficient increases when the values of the unsteadiness parameter increase. Also, it is observed as expected from Table 1 that the modified skin friction coefficient is strongly influenced by the presence of a strong magnetic field. The implication of this is that application of a strong magnetic field perpendicular to the field flow provides a drag force that retards the flow thereby increasing the friction on the wall surface. Furthermore, in Table 1, we found that the modified skin friction coefficient increase with increasing value of suction. Fig. 1 displays the effects of suction and blowing on the velocity distribution for thermal buoyancy. It is clearly observed that an increase in convection due to thermal buoyancy parameter the fluid velocity is accelerated. Also, injecting fluid into the fluid flow increases the fluid while suction decelerate the fluid flow which validates known results (Shateyi *et al.* [8]). It is good to remark that mass convective parameter has similar effect on the velocity profiles.

Table 1. Comparison of $f''(0)$, $\theta'(0)$ and $\phi'(0)$ for RKF45 and MMRE when $Gc_\xi = Gr_\xi = 0$, $\beta \to \infty$.

Parameters			$-f''(0)$			Present Results (MMRE)		
A	M	f_w	Mansur and Ishak [36]	Butt and Ali [37]	Shateyi [21] (Rkf45)	$-f''(0)$	$-\theta'(0)$	$-\phi'(0)$
0.0	1.0	0.5	-	1.68614	1.68614	1.6861405	0.3300713	1.9055148
0.5			-	1.80242	1.80242	1.8024223	0.5728878	2.0855039
1.0			-	1.91407	1.91407	1.9140705	0.7355349	2.2496063
1.5			-	-	2.02081	2.0208144	0.8659487	2.4013006
2.0			-	2.12280	2.12280	2.1228029	0.9779791	2.5430358
0.5	0.0	0.5	-	1.43132	1.43132	1.4313245	0.8044079	2.1257205
	0.5		-	1.63018	1.63018	1.6301795	0.6780084	2.1035733
	1.0		-	1.80242	1.80242	1.8024223	0.5728878	2.0855039
	1.5		-	1.95686	1.95686	1.9568579	0.4814416	2.0701108
	2.0		-	2.09818	2.09818	2.0981799	0.3997565	2.0566566
0.0	1.0	0.0	-	1.53905	1.53905	1.5390514	0.5348540	1.8343983
		0.5	-	1.80242	1.80242	1.8024223	0.5728878	2.0855039
		1.0	-	2.10567	2.10567	2.1056663	0.6175234	2.3713178
		1.5	-	2.44537	2.44537	2.4453733	0.6704366	2.6907319
		2.0	-	2.81623	2.81623	2.8162342	0.7320629	3.0406515
0.0	0.0	2.0	2.4142	-	2.41421	2.4142134	0.7260575	2.9177104
		2.5	2.8508	-	2.85078	2.8507808	0.7906384	3.2998521
		3.0	3.3028	-	3.30277	3.3027753	0.8646242	3.7046905

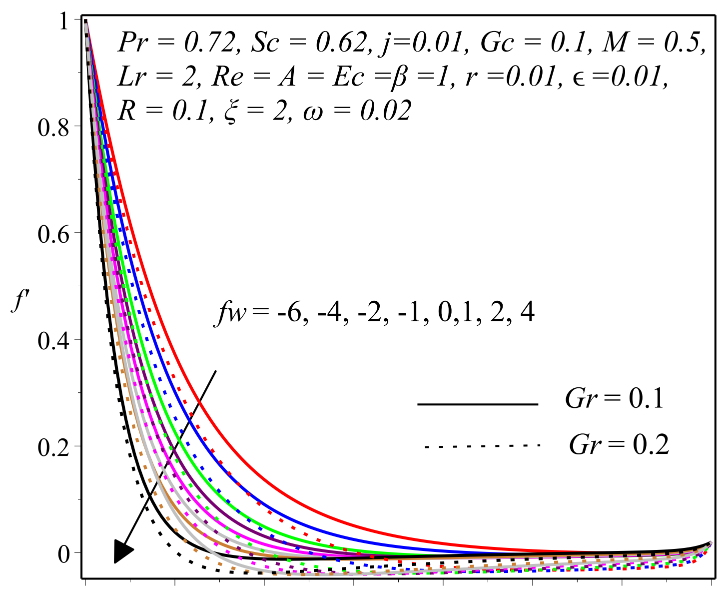

FIGURE 1. f' vs η for some fw and Gr

Fig. 2 shows that the effects of the Eckert number with the variation of thermal radiation on the velocity distribution. The presence of viscous dissipation causes heat generation, which in turn accelerates the fluid flow. It is also found that increasing values of the Eckert number causes increase in the velocity profiles. In the same vein, the presence of thermal radiation increases the flow because heat is already in the system though there is heat loss due to thermal radiation.

It is observed from Fig.3 that the velocity decreases with increasing values of the Casson parameter leading to decrease in the fluid stress and suppresses the velocity. The velocity is also observed to decrease with increase in the values of unsteadiness parameter. In Fig. 4, the effect of streamwise parameter is presented with the velocity power law exponent. It is observed that the velocity distribution decreases with increase in streamwise parameter (ξ) and then smoothened by higher streamwise parameter which some authors have actually neglected by setting it to 0 limiting the solution to self similar case. On the contrary, the velocity profile increases with increase in velocity power law exponent (j).

Fig. 5 depicts the effect of increase in magnetic field parameter and solutal Grashof number on the velocity profiles. The presence of a magnetic field induces a current in the conductive fluid, and then

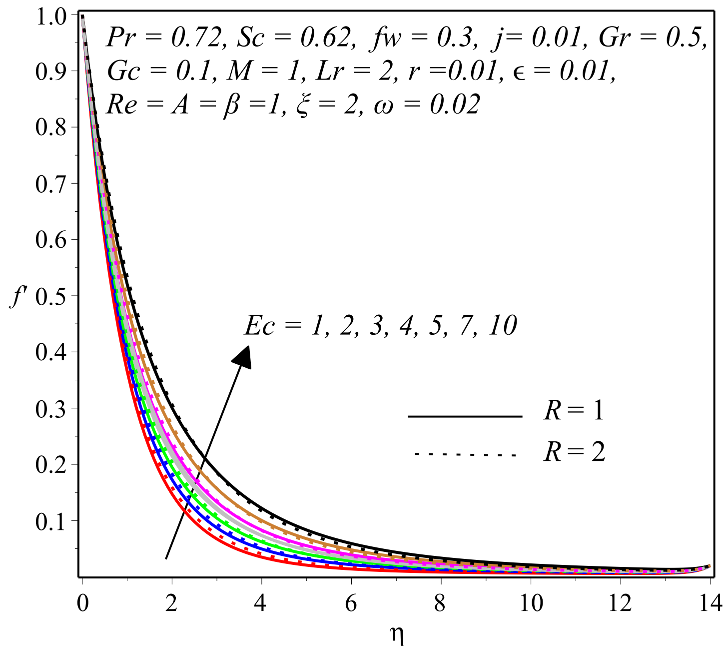

FIGURE 2. f' vs η for some Ec and R

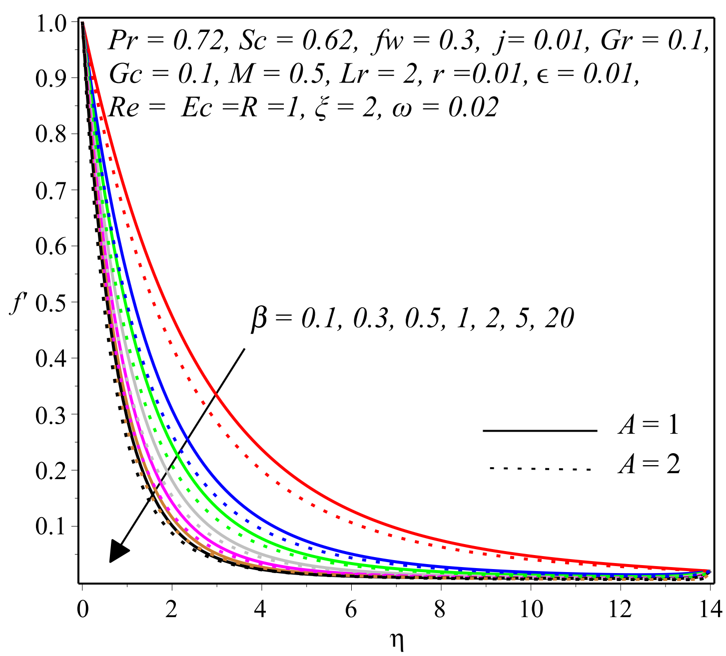

FIGURE 3. f' vs η for some β and A

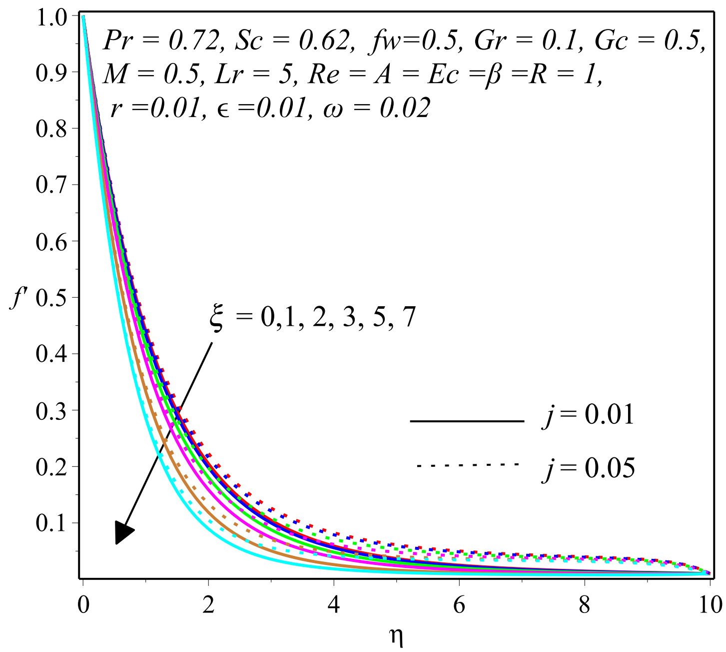

FIGURE 4. f' vs η for some ξ and j

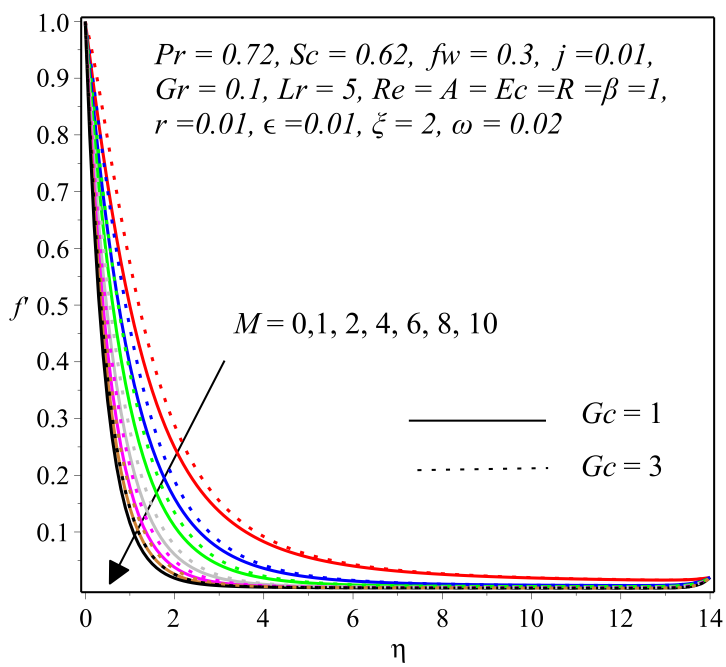

FIGURE 5. f' vs η for some M and Gc

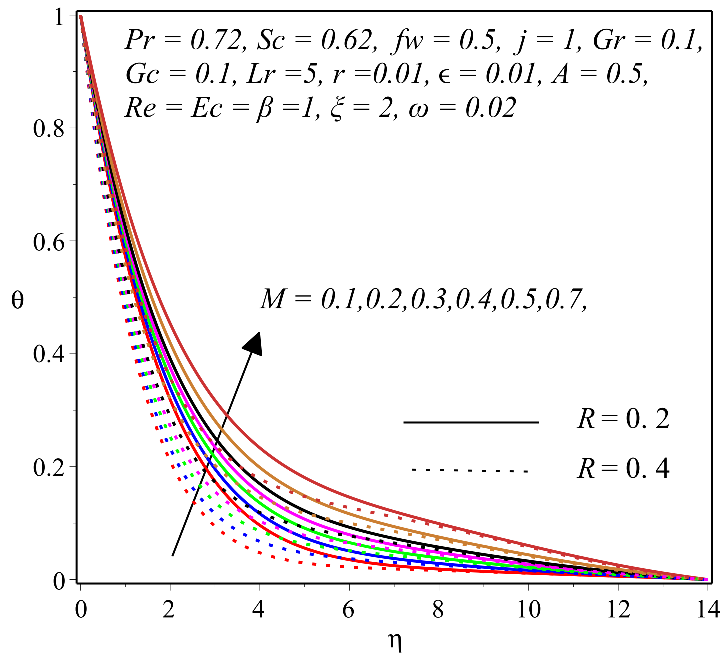

FIGURE 6. θ vs η for some M and R

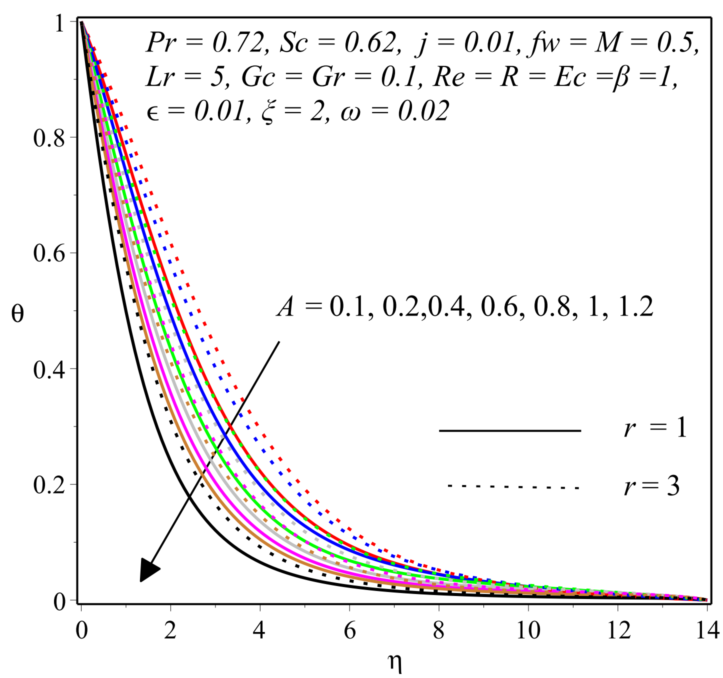

FIGURE 7. θ vs η for some A and r

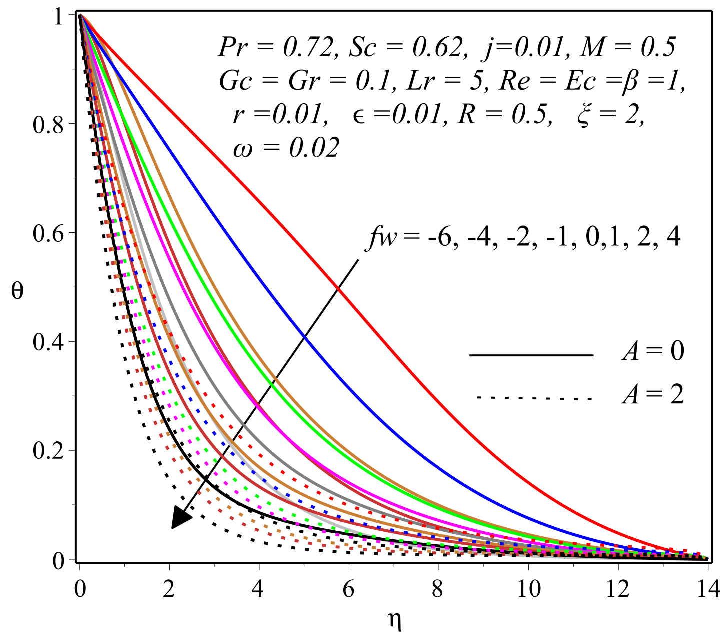

FIGURE 8. θ vs η for some fw and A

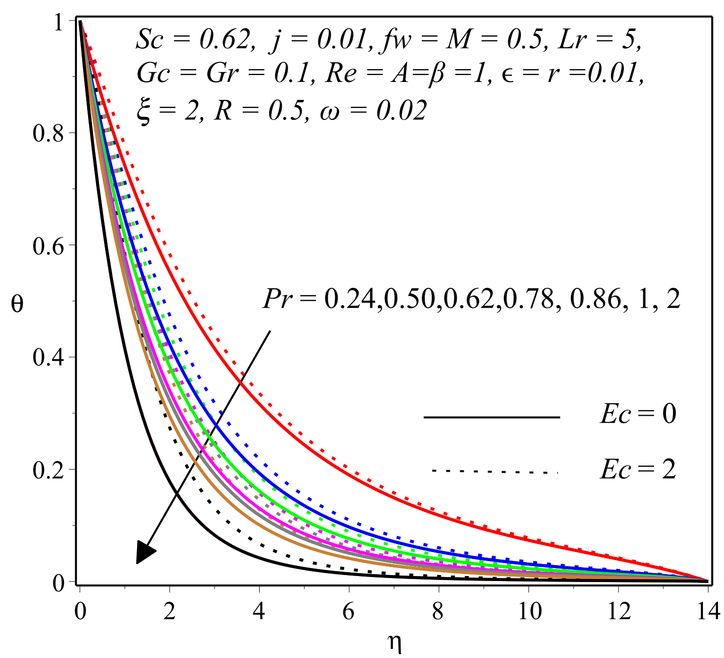

FIGURE 9. θ vs η for some Pr and Ec

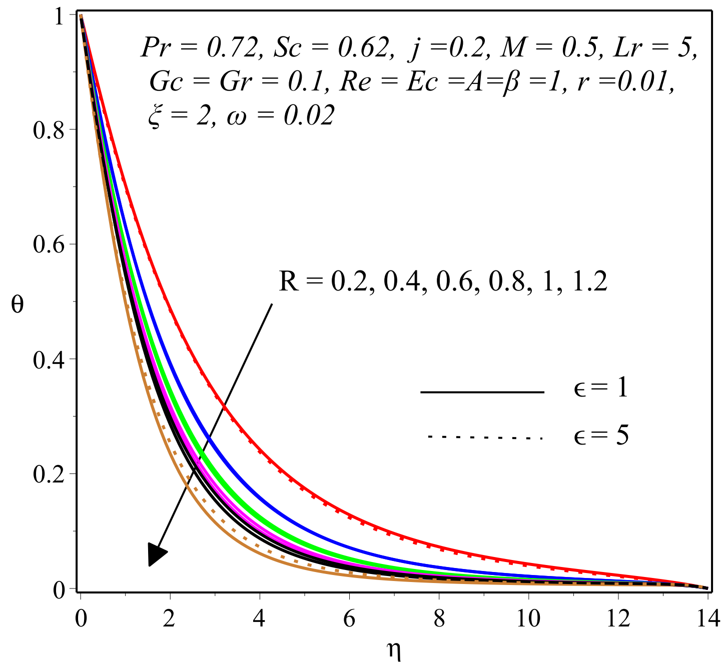

FIGURE 10. θ vs η for some R and ϵ

creates a resistive-type of force on the fluid in the boundary layer, which slows down the motion of the fluid. The implication is that magnetic field can consequently be used to control boundary layer separation. It is observed that the solutal Grashof number enhances the velocity profiles.

Fig. 6 shows that the presence of a magnetic field strength parameter and thermal radiation on the temperature profiles. The temperature rises with increasing values of magnetic field strength parameter. This is because the applied magnetic field enhances friction which tends to heat the fluid and therefore leads to an increase in temperature. Asogwa and Ibe [35] reported similar observation for the influence of magnetic field in an electrically conducting fluid flow and temperature profiles. It is also observed that the increase in thermal radiation reduces the temperature profiles.

Fig. 7 depicts the influence of unsteadiness parameter as well as the variable thermal conductivity on the temperature profiles. It is noted that the fluid temperature is reduced by increasing value of unsteadiness parameter as reported by Shateyi [8]. On the contrary, the increase in variable thermal conductivity parameter is found to have caused a distinct increase in the temperature profile.

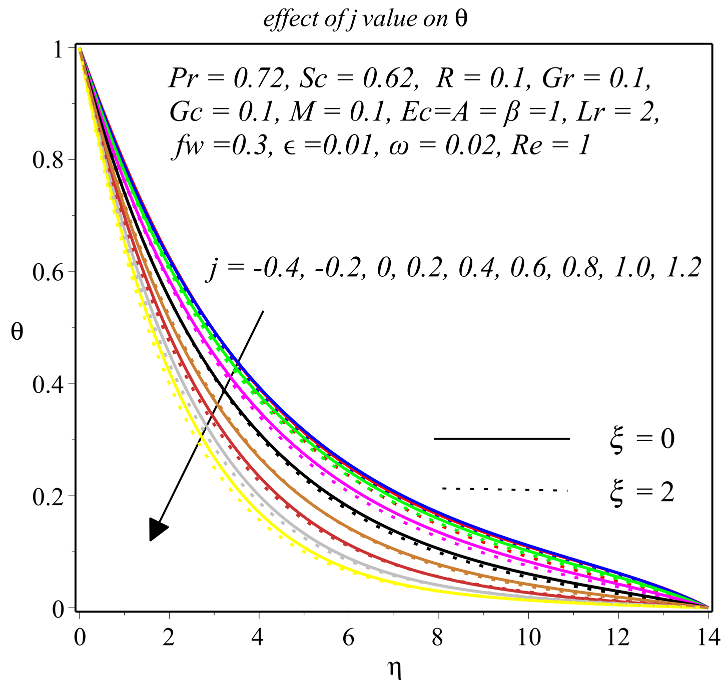

FIGURE 11. θ vs η for some j and ξ

Fig. 8 shows the effects of suction/injection as well as unsteadiness parameter on the temperature profiles. It is observed that increase in suction/injection parameter reduces the fluid temperature profiles. Also, when the unsteadiness parameter is zero implies the steady state and the temperature profiles are exceptionally high while the temperature profiles are drastically reduced when the unsteadiness parameter is nonzero (e.g. $A = 2$) which is the unsteady state.

The presence of viscous dissipation significantly influence the temperature profiles as shown in Fig. 9. This is evident as increase in Eckert number leads to increase in temperature, which is in agreement with Khan *et al*. [34]. The effects of Prandtl number Pr is also displayed in Fig. 9. It is observed that an increase in Prandtl number leads to the reduction in the temperature. This behaviour is as a result of Pr being strongly dependent on thermal diffusivity of fluid from the definition $Pr = \frac{\mu}{\alpha}$, meaning that larger Pr has weaker thermal diffusivity which is responsible for a reduction in temperature. This finding supports the report of Olanrewaju *et al*. [36] that increase in Prandtl number decreases the temperature profile and thereby decreases the

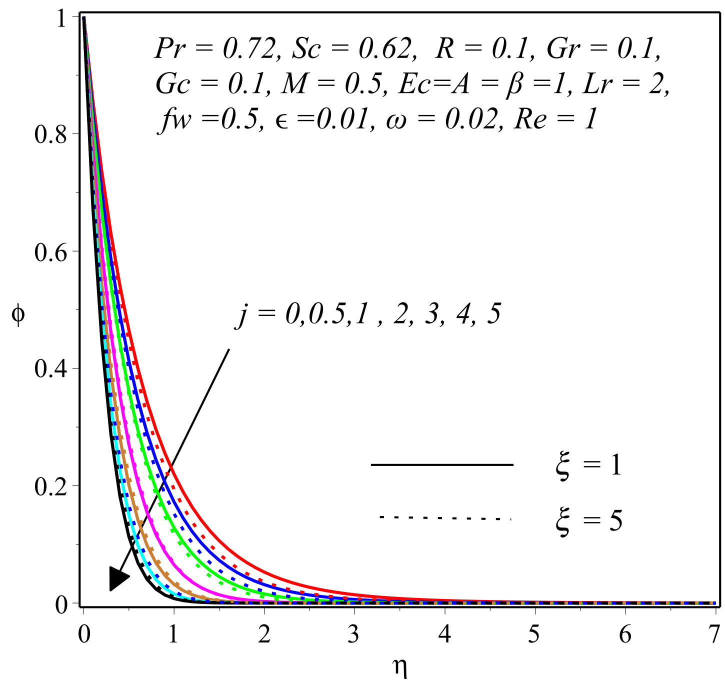

FIGURE 12. ϕ vs η for some j and ξ

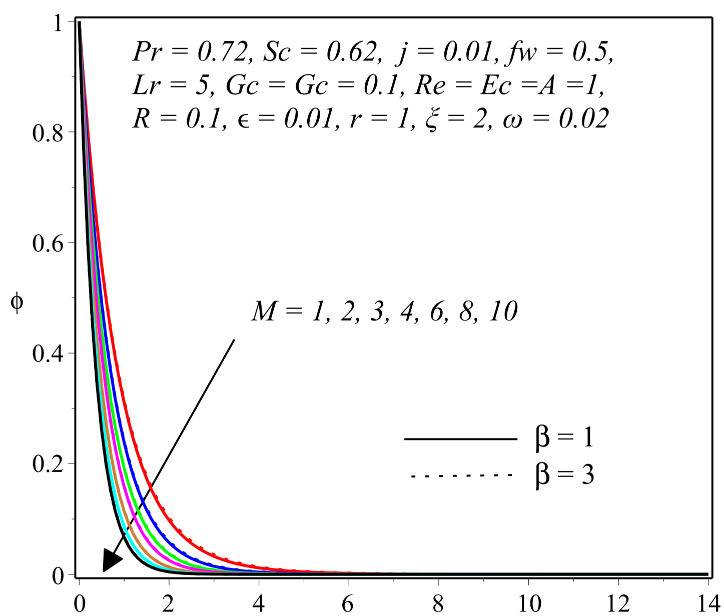

FIGURE 13. ϕ vs η for some Lr and β

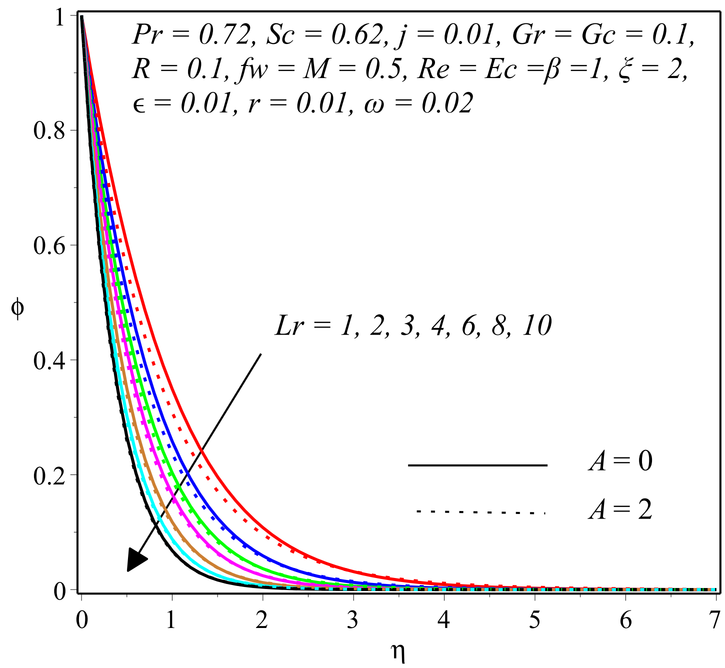

FIGURE 14. ϕ vs η for some Lr and A

thermal boundary layer thickness leading to thinner boundary layer which is in agreement with Rao *et al*. [37]. Also, the observation in this result corroborate what is in literature as reported by Koriko *et al*. [38]. The same Fig. 9 shows the strength of Ec, but on the contrary, the dissipation phenomenon triggers to produce extra heat associated with the frictional heating among the particles of fluid which leads to boosting of the temperature profile as reported by Khan [34]. The effect of variable viscosity parameter is also presented in Fig. 10. It is clearly observed that the lower the value of variable viscosity parameter the better the temperature profile, higher values make the profiles closely packed.

Fig. 11 displays the variation of pressure gradient (in terms of velocity power law exponent j) on fluid temperature in that the temperature profiles for $j > 0$ is higher than $j < 0$. This is because for a positive value of j, pressure gradient is negative and for a negative value of j, pressure gradient is positive $\left(-\frac{1}{\rho}\frac{\partial P}{\partial x} = U_e\frac{dU_e}{dx} = j\frac{\lambda a^2 x^{2j-1}}{(1-ct)^2}\right)$, when $U_e = \frac{\lambda a x^j}{(1-ct)^2}$ according to Kundu *et al*. [26]. In the case of

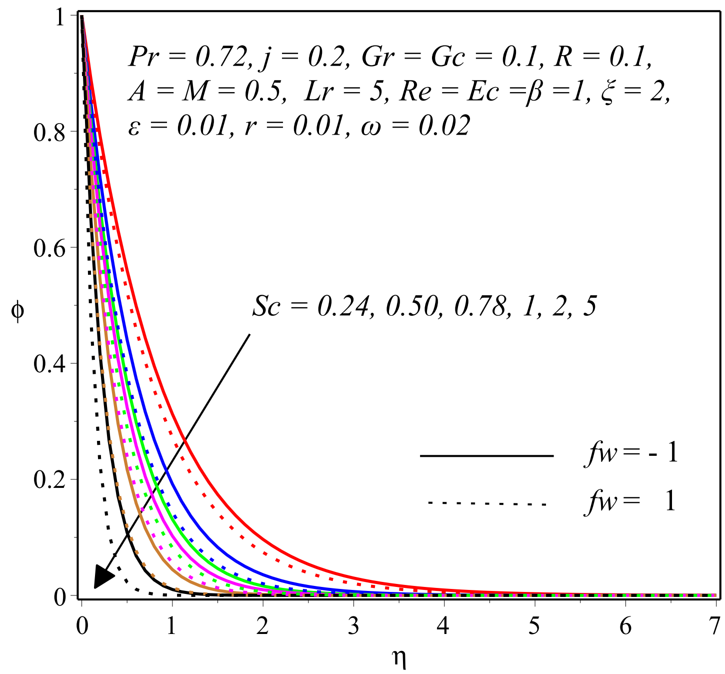

FIGURE 15. ϕ vs η for some Sc and fw

accelerating flows ($j > 0$), the velocity profiles have no points of inflection, whereas in the case of decelerated flows ($j < 0$) which corroborate Fig. 3. According to Rosales-Vera and Valencia [39], the physical relevant solutions exist only for $-0.19884 < j \leq 2$. A negative pressure gradient is as a result of pressure decrease in the direction of fluid flow across the boundary layer. Thus the fluid within the boundary layer has enough momentum to overcome the resistance which is trying to push it backward and the flow accelerates. For a positive pressure gradient the pressure increases in the direction of flow, the fluid within the boundary layer has little momentum to overcome this resistance which could make the flow to be retarded and possibly lead to flow reversal. The above explanation accounts for the similar behaviour in Fig. 12 and then smoothened by higher streamwise parameter which some authors have actually neglected by setting it to 0 limiting the solution to self similar case. Beg *et al*. [40] is also in support of Figs. 11 and 12.

Fig. 13 shows the effects of magnetic strength and Casson parameters on the concentration profiles. It is observed that increase in magnetic strength parameter reduces the concentration profiles. This may be due to friction which generating more heat energy that eventually increases the temperature distribution in the flow and therefore the concentration reduces with increase in magnetic strength parameter. Similarly increase in Casson fluid parameter increase the concentration profiles.

Fig. 14 presents the influence of variation of chemical reaction parameter on the concentration profiles at different values of unsteadiness parameter. It is noticed that increase in chemical reaction parameter reduces the concentration profiles which is physically reasonable. The effect of variation of A is also observed in that the steady state increase the concentration profiles and converse is true for the unsteady state.

Fig. 15 displays the influence of Sc on ϕ, it can be seen that the presence of heavier species (high Schmidt number) reduces the concentration profiles. Similar report is given by Awais *et al.* [41].

4. CONCLUDING REMARKS

The current study is a theoretical analysis of a two-dimensional unsteady laminar boundary layer, heat and mass transfer of an incompressible Casson fluid over a stretching sheet in the presence of viscous dissipation, variable viscosity and thermal conductivity. The research questions have been answered by this study and the following concluding remarks are drawn:

- The contributions of variable viscosity and thermal conductivity are very significant and notable on Casson fluid by increasing velocity and temperature profiles.
- The influence of nonlinear stretching velocity from exponent is much felt on the fluid velocity by increasing its profiles while it causes decrease in temperature and concentration profile; and
- The presence of the independent variable x in A, Gr_x, Gc_x and Lr justifies the need for the Local Nonsimilarity Solution Approach which is capable of handling such parameters with error. Moreover, Local Nonsimilarity Solution Approach provides full solution and never truncated at the first level of truncation or solution like other in literature work.
- The increase in magnetic field reduces the velocity and concentration profiles but the magnetic field and Prandtl number enhances the temperature.
- An increase in suction parameter reduces velocity and concentration profiles.

- The heat and mass transfer is reduced with the magnetic parameter, Prandtl number, Schmidt number buoyancy and chemical reaction parameters.

ACKNOWLEDGEMENTS

The authors would like to thank the anonymous referees whose comments improved the original version of this manuscript.

NOMENCLATURE

a, b, c	initial stretching rate, stretching rate, positive constant respectively,
A_x	ratio of stretching rate or unsteadiness parameter,
B_o	applied uniform transverse magnetic field strength,
C	dimensional species concentration of the fluid,
C_w	species concentration of the fluid along the sheet wall,
C_∞	species concentration of the fluid far away from the sheet wall,
C_p	specific heat capacity at constant pressure,
D_m	effective diffusive coefficient or mass diffusion coefficient,
E	activation energy,
Ec	Eckert number,
f	dimensionless or reduced stream function,
f'	dimensionless axial velocity variable,
F	auxiliary velocity function, $\dfrac{\partial f}{\partial \xi}$,
g^*	acceleration due to gravity
G	auxiliary velocity function, $\dfrac{\partial F}{\partial \xi}$,
Gr_x	local thermal Grashof number
Gc_x	local Solutal Grashof number
H	auxiliary temperature function, $\dfrac{\partial X}{\partial \xi}$,
K_T	thermal diffusion ratio
Lr	chemical reaction parameter
M	Magnetic strength parameter/Local Hartmann number
P	pressure
Pr	Prandtl number
r	variable viscosity parameter
R	thermal radiation parameter
R^*	universal gas constant
Re_x	local Reynolds number

S	auxiliary dimensionless concentration function, $\dfrac{\partial Y}{\partial \xi}$,
Sc	Schmidt number
t	time
T	dimensional temperature of the fluid
T_m	mean fluid temperature
T_w	temperature of the sheet wall
T_∞	dimensional or free stream temperature of the fluid far away from the sheet
u, v, w	velocity components in x, y and z direction respectively
U_w	velocity at the sheet wall or mainstream velocity
U_∞	velocity far away from the sheet wall or free stream velocity
X	auxiliary dimensionless temperature function, $\dfrac{\partial \theta}{\partial \xi}$,
Y	auxiliary dimensionless concentration function, $\partial\phi/\partial\xi$,

Greek Symbols

α	thermal diffusivity
β_T	thermal expansion(volumentric) coefficient
β_c	concentration expansion coefficient
δ	heat source/sink parameter
ϵ	variable thermal conductivity parameter
η	pseudo-similarity variable
μ	dynamic viscosity
ν	kinematic fluid viscosity
κ	constant thermal conductivity
θ	dimensionless temperature
ϕ	dimensionless concentration
ρ	fluid density
σ	electrical conductivity of fluid
ξ	non-similarity variable
ω	is the ratio of stretching rate of free stream velocity and velocity at the wall

Subscripts and Superscripts

w	condition at the wall
j	exponent of nonlinear stretching velocity/streamwise pressure gradient parameter.

REFERENCES

[1] C. Sumalatha and S. Bandari, *Effects of Radiations and Heat Source/Sink on a Casson Fluid Flow over Nonlinear Stretching Sheet*, World Journal of Mechanics, **5**, (2015), 257-265.

[2] M. Nakamura and T. Sawada, *Numerical Study on the Flow of a Non-Newtonian Fluid through an Axisymmetric Stenosis*, ASME J Biomechanical Eng, **110**, (1988), 137-143.

[3] N. Casson, *Rheology of Disperse Systems in Flow Equation for Pigment Oil Suspensions of the Printing Ink Type*, Rheology of Disperse Systems, Mill, C. C., Ed., London: Pergamon 1959, 84-102.

[4] M. Mustafa , Hayat T., Pop I. and Aziz A. *Unsteady Boundary Layer Flow of a Casson Fluid Due to an Impulsively Started Moving Flat Plate*, Heat TransferAsian Research, **40**(6), (2011), 563-576.

[5] R. K. Dash , K. N. Mehta and G. Jayaraman, *Casson Fluid Flow in a Pipe Filled with a Homogeneous Porous Medium*, Int J Eng Sci, **34**(10), (1996), 1145-1156.

[6] S. Mukhopadhyay, I. C. Moindala and T. Hayat, *MHD Boundary Layer Flow of Casson Fluid passing through an Exponentially Stretching Permeable Surface with Thermal Radiation*, Chinese Physical Society, **23**(10), (2014), 1-9.

[7] S. Mukhopadhyay, *Casson Fluid Flow and Heat Transfer over a Nonlinearly Stretching Surface*, Chinese Physical Society, **22**(7), (2013), 1-5.

[8] S. Shateyi, F. Mabood and G. Lorenzini, *Casson Fluid Flow: Free Convective Heat and Mass Transfer over an Unsteady Permeable Stretching Surface Considering Viscous Dissipation*, Journal of Engineering Thermophysics, **26**(1), (2017), 39-52.

[9] S. Nadeem, R. U. Haq, N. S. Akbar and Z. H. Khan, *MHD Three-dimensional Casson Fluid Flow past a Porous Linearly Stretching Sheet*, Alexandria Engineering Journal, **52**, (2013), 577-582.

[10] S. Pramanik, *Casson Fluid Flow and Heat Transfer past an Exponentially Porous Stretching Surface in Presence of Thermal Radiation*, Ain Shams Engineering Journal, **5**, (2014), 205-212.

[11] K. Ramesh and M. Devakar, *Some Analytical Solutions for Flows of Casson Fluid with Slip Boundary Conditions*, Ain Shams Engineering Journal, **6**, (2015), 967-975.

[12] Md. Afikuzzaman and A. Md. Mahmud, *MHD Casson Fluid Flow through a Parallel Plate*, Thammasat International Journal of Science and Technology, **21**(1), (2016), 59-70.

[13] E. M. Arthur, I.Y. Seini and L. B. Bortteir, *Analysis of Casson Fluid Flow over a Vertical Porous Surface with Chemical Reaction in the Presence of Magnetic Field*, Journal of Applied Mathematics and Physics, **3**, (2015), 713-723.

[14] F. M. White, *Viscous Fluid Flow*, Third Edition, McGraw-Hill, New York, (2006), 146 - 147.

[15] E. M. Sparrow, H. Quack and C. J. Boerner, *Local Non-similarity Boundary Layer Solutions*, American Institute of Aeronautics and Astronatics Journal, **8**(11), (1970), 1936 - 1942.

[16] R. Mohamad, R. Kandasamy and M. Ismoen, *Local Non-similarity Solution for MHD Mixed convection Flow of a Nanofluid Past a Permeable Vertical Plate in the Presence of Thermal Radiation Effects*, Journal of Applied and Computational Mathematics, (2015), **4**(6), 1 - 9.

[17] F. S. Ibrahim and I. A. Hassanien, *Local nonsimilarity solutions for mixed convection boundary layer flow of a micropolar fluid on horizontal flat plates with variable surface temperature*, Applied Mathematics and Computation, **122**, (2001), 133-153.

[18] P. M. Patil, D. N. Latha, S. Roy and E. Momoniat, *Non-similar solutions of mixed convection flow from an exponentially stretching surface*, Ain Shams Engineering Journal, **8**, (2017), 697-705.

[19] I. L. Animasaun, E. A. Adebile and A. I. Fagbade, *Casson Fluid Flow with Variable Thermo-physical Property along Exponentially Stretching Sheet with Suction and Exponentially Decaying Internal Heat Generation using the Homotopy Analysis Method*, Journal of the Nigerian Mathematical Society, **35**, (2016), 1-17.

[20] K. Bhattacharyya, *Effects of Heat Source/Sink on MHD Flow and Heat Transfer over a Shrinking Sheet with Mass Suction*, Chemical Engineering Research Bulletin, **15**, (2011), 12–17.

[21] I. L. Prasad, E. A. Adebile and A. I. Fagbade, *Casson Fluid Flow with Variable Thermo-physical Property along Exponentially Stretching Sheet with Suction and Exponentially Decaying Internal Heat Generation using the Homotopy Analysis Method*, Journal of the Nigerian Mathematical Society, **35**, (2016), 1-17.

[22] W. J. Minkowycz and E. M. Sparrow, *Numerical Solution scheme for Local Nonsimilarity Boundary Layer Analysis*, Numerical Heat Transfer, **1**, (1978), 69 - 85.

[23] E. M. Sparrow and H. S. Yu, *Local Non-similarity Thermal Boundary Layer Solutions*, Journal of Heat Transfer, **93**, (1971), 328 - 334.

[24] A. Ishak,R. Nazar and I. Pop, *Heat Transfer over an Unsteady Stretching Permeable Surface with Prescribe Wall Temperature*, Nonlinear Analysis: Real World applications, **10**, (2009), 2909-2913.

[25] S. Khan,I. Karim and H. A. Biswas, *Heat generation, thermal radiation and chemical reaction effects on MHD mixed convection flow over an unsteady stretching permeable surface*, International Journal of Basic and Applied Science, **1**(2), (2012), 350 - 364.

[26] P. K. Kundu and I. M. Cohen, *Fluid Mechanics.* Fourth edition, Elsevier, The Boulevard, Langford lane Kidlington, Oxford, UK (2008), ISBN: 978-0-12-373735-9.

[27] M. O. Lawal and S. O. Ajadi, *Local nonsimilarity solutions for mixed convective flow over a stretching sheet in the presence of chemical reaction and Hall current*, Journal of the Nigerian Mathematical Society, **39**(3), 353-388, 2020.

[28] T. Thumma, A. Wakif and I. L. Animasaun, *Generalized differential quadrature analysis of unsteady three-dimensional MHD radiating dissipative Casson fluid conveying tiny particles*, Heat Transfer, **49**(5), 2595-2626, 2020.

[29] M. A. Hossain, K. Khanafer and K. Vafai, *The Effect of Radiation on Free Convection Flow of Fluid with Variable Viscosity from a Porous Vertical Plate*, Int. J. Therm. Sci., **40**(2), (2001), 115-124.

[30] S. Mansur and A. Ishak, *The Flow and Heat Transfer of a Nanofluid past a Stretching/Shrinking Sheet with Convective Boundary Condition.* Abst. Appl. Anal. , **2013**, (2013), 1-9.

[31] T. E. Akinbobola and S. S. Okoya, *The flow of second grade fluid over a stretching sheet with variable thermal conductivity and viscosity in the presence of heat source/sink*, Journal of the Nigerian Mathematical Society, **34**, 331-342, 2015.

[32] R. C. Bataller, *Effects of heat source/sink, radiation and work done by deformation on flow and heat transfer of a viscoelastic fluid over a stretching sheet.* Comput Math Appl **53**, 305-316, 2007.

[33] E. O. Fatunmbi, S. S. Okoya and O. D. Makinde, *Convective heat transfer analysis of hydromagnetic micropolar fluid flow past an inclined nonlinear stretching sheet with variable thermophysical properties*, Diffusion Foundations, ISSN: 2296-3642, **26**, (2020), 63-77.

[34] M. R. Khan, M. A. Elkotb, R. T. Matoog, N. A. Alshehri and M. A. H. Abdelmohimen, *Thermal feature and heat transfer enhancement of a Casson fluid across a porous stretching/shrinking sheet: Analysis of dual solution*, Case studies in Thermal Engineering, **28**, 101594, 2021.

[35] K. K. Asogwa and A. A. Ibe, *A study of MHD Casson fluid flow over a permeable stretching sheet with heat and mass transfer*, Journal of Engineering Research and Report, **16**(12): 10-25, 2020.

[36] P. O. Olanrewaju, A. W. Ogunsola, D. A. Ajayi and S. A. Bishop, *Effect of chemical reaction thermal radiation, internal heat generation, soret and dufour on chemically reacting MHD boundary layer flow of heat and mass transfer past a moving plate with suction/injection*, Federal University of Wukari Trends in Science and Technology Journal, **1**(1), (2016), 145 - 153.

[37] G. S. Rao, B. B. Ramana, R. Reddy, and G. Vidyasagar, *Soret and Dufour effects on MHD boundary layer flow over a moving vertical porous plate with suction*, International Journal of Emerging Trends in Engineering and Development, **2**(4), (2014), 215 - 226.

[38] O. K. Koriko, J. A. Omowaye and I. L. Animasaun, *Effects of some thermophysical parameters on free convective heat and mass transfer over vertical stretching surface at absolute zero*, Journal of Heat and Mass Transfer Research, **1**, (2016), 31 - 46.

[39] M. Rosales-Vera and A. Valencia, *Solutions of Falkner-Skan equation with heat transfer by Fourier series*, International Communications in Heat and Mass Transfer, **37**, (2010), 761-765.

[40] O. A. Beg, T. A. Beg, A. Y. Bakier, and V. R. Prasad, *Chemically-reacting mixed convective heat and mass transfer along inclined and vertical plates with Soret and Dufour effects: numerical solutions*, Int. J. of Appl. Math and Mech. **5**(2): 39-57, 2009.

[41] M. Awais, M. A. Raja, S. E. Awan, M. Shoaib and H. M. Ali, *Heat and mass transfer phenomenon fro the dynamics of Casson fluid through porous medium over shrinking wall subject to Lorentz force and heat source/sink*, Alexandria Engineering Journal, **60**(1), 1355-1363, 2021.

DEPARTMENT OF MATHEMATICS, ADEYEMI COLLEGE OF EDUCATION, ONDO, NIGERIA
E-mail address: `femathlaw@yahoo.com`

DEPARTMENT OF MATHEMATICS, OBAFEMI AWOLOWO UNIVERSITY, ILE - IFE, NIGERIA
E-mail addresses: `sajadi@oauife.edu.ng`